

Cu-based quaternary chalcogenide $\text{Cu}_2\text{BaSnS}_4$ thin films acting as hole-transport layers in inverted perovskite $\text{CH}_3\text{NH}_3\text{PbI}_3$ solar cells

Jie Ge, Corey R. Grice, and Yanfa Yan

Department of Physics and Astronomy & Wright Center for Photovoltaics Innovation and Commercialization, the University of Toledo, Toledo, Ohio 43606, United States

Experimental Section

Materials synthesis and device fabrication:

Cu₂BaSnS₄ (CBTS): CBTS precursor films were deposited on commercial fluorine-doped SnO₂ (FTO) glass (TEC 15, NSG) substrates by co-sputtering Cu, SnS and BaS targets (3 in., Plasma Materials Co.) using the LAB Line SPUTTER 5 system (Kurt J Lesker Co.). The substrate temperature was kept at 150 °C during the co-sputtering. The Cu poor composition of film precursors was controlled by varying the radio-frequency powers for each target, Cu: 45W; SnS: 45 W; BaS: 110 W. The co-sputtered precursor films were then annealed in sulfur vapor at 540 °C for 30 min to yield the CBTS with the desirable *p*-type conductivity. The film thickness was adjusted by varying the cosputtering deposition time: 100 nm for 5 min; 150 nm for 8 min; 500 nm for 30 min. The sulfurized CBTS films were dipped in a 1 M KCN aqueous solution for 30 s, followed by deionized water and methanol rinsing for 2 min and drying with nitrogen.

CH₃NH₃PbI₃ (MaPbI₃): The perovskite precursors were prepared by spin-coating the precursor solution consisting of 461 mg of PbI₂ and 159 mg of CH₃NH₃I dissolved in 723 μ L of N,N-dimethylformamide and 81 μ L of dimethyl sulfoxide. The molar ratio between PbI₂ and CH₃NH₃I is 1:1. All the perovskite precursors were annealed at 60 °C for 2 min and then 120 °C for 15 min in a glovebox.

Phenyl-C₆₁-butyric acid methyl ester (PCBM): PCBM films were spin-coated using 10 mg mL⁻¹ PCBM dichlorobenzene solutions with a spin rate of 2000 rpm for 30 s and then annealed on a hotplate at 100 °C for 10 min in a glove box.

2,20,7,70-tetrakis-(N,N-di-pmethoxyphenylamine) 9,90-spirobifluorene (Spiro): The Spiro solution consisted of 26 mM Li-bis(trifluoromethanesulfonyl) imide (LiTFSI) (Sigma, 99.95%), 55 mM 4-tert-butylpyridine (TBP), and 68 mM Spiro, which were dissolved in a mixed solvent of acetonitrile and chlorobenzene with a volume ratio of 1:10. The Spiro solution was spin-coated on the perovskite films at 500 rpm for 1 s and subsequently 2000 rpm for 60 s in a dry box.

Poly (3,4-ethylenedioxythiophene): poly(styrene sulfonate) (PEDOT:PSS): PEDOT:PSS (Baytron 4083) was then spin-cast onto clean FTO substrates, followed by annealing at 150 °C for 10 min in air.

TiO₂: a compact TiO₂ blocking layer was spin-coated with 0.3 M titanium diisopropoxide bis(acetylacetonate) in 1-butanol solution by the spin-coating method, which was heated at 200 °C for 15 min. On the prepared compact TiO₂ blocking layer, the nanocrystalline TiO₂ paste (Dyesol) diluted with ethanol was spin-coated and the deposited film was annealed at 550 °C for 1 h to produce mesoporous TiO₂ thin layer.

Metal electrode: 60 nm thick Au and Ag electrodes were thermally evaporated on top of Spiro and PCBM, respectively. The total area of the solar cells was 0.08 cm².

Film characterization:

X-ray diffraction (XRD) data were collected using a Rigaku Ultima III diffractometer with Cu K α lines (0.15418 nm) in Bragg-Brentano Theta-2Theta scans, with the Cu source

operated at 40 kV and 44 mA electron excitation current. Theta calibration was done using a standard Si sample prior to the measurements. The phase identification and the refinement of lattice constants were done using the software of MDI Jade 2010 equipped with a monthly synchronized ICDD database (International Centre for Diffraction Data). Confocal Raman spectroscopy was carried out using a 632.8 nm laser (HORIBA Scientific), with the Raman shift calibrated by a Si sample at 520.4 cm⁻¹. The optical transmittance of a CBTS thin film deposited on a FTO substrate was measured by an ultraviolet–visible spectrophotometer (PerkinElmer Lambda 1050). The composition of our CBTS thin films were characterized by energy dispersive X-ray spectroscopy (EDS) equipped in a field–emission scanning electron microscope (FE–SEM) (Hitachi S4800 FE–SEM).

To determine the band positions of CBTS, we performed the dark capacitance-voltage (C-V) measurement in a neutral electrolyte (pH=6.4) containing sodium sulfite (0.5 M) and potassium phosphate (0.5 M) based on 3-electrode configuration, where FTO/CBTS serves as the working electrode, a Ag/AgCl (1 M KCl) electrode serves as the reference electrode, and a Pt wire serves as the counter electrode. A photoelectrochemistry workstation equipped with a frequency analyzer (ModuLab, Solartron Analytical) was used for this measurement. Potentials versus the Ag/AgCl (1 M KCl) electrode ($E_{\text{Ag/AgCl}}$) were converted to potential versus reversible hydrogen electrode (RHE, V_{RHE}) using the Nernst equation, namely, $V_{\text{RHE}} = V_{\text{Ag/AgCl}} + 0.059 \times \text{pH} + 0.222$.

Device Testing:

The J – V curves of the perovskite solar devices measured under a simulated AM1.5G irradiation with a standard solar simulator (PV Measurements Inc.). The EQE data were measured using a commercial EQE system (PV Measurements Inc.). EQE derived photocurrent/short circuit current densities (J) can be integrated from the expression

$$J = \frac{e}{hc} \int \lambda (\text{EQE} * \text{AM1.5G}) d\lambda$$

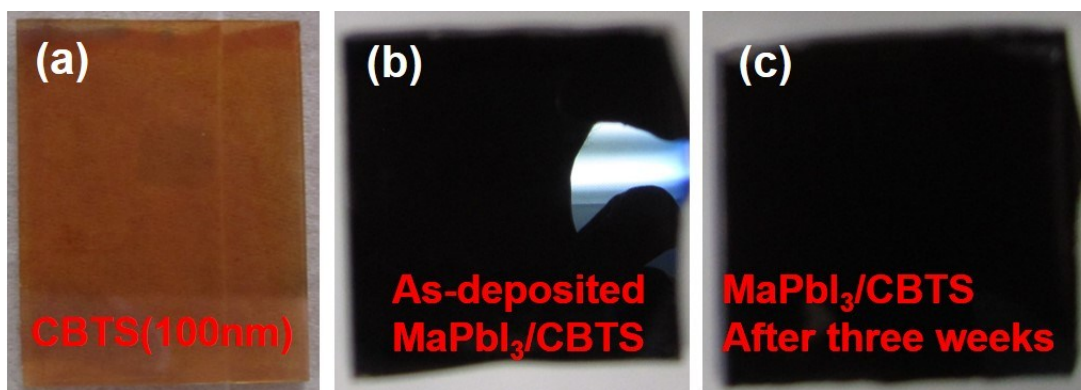


Figure S1 Digital photos of a 100 nm thick CBTS film (a), a just-made MaPbI₃ film on CBTS (b), and a MaPbI₃/CBTS sample which was stored in a N₂ filled desiccator for three weeks.

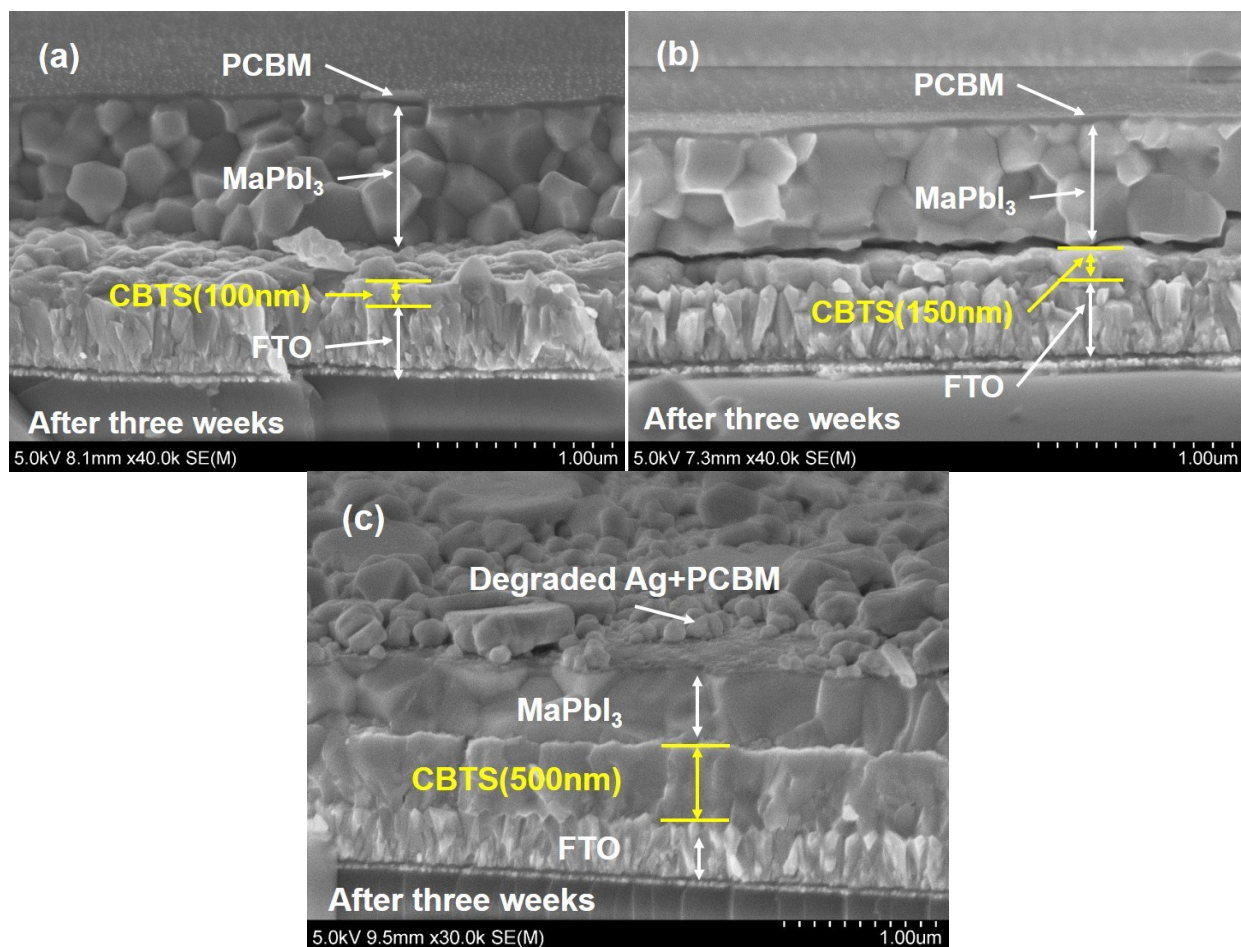


Figure S2 Cross-sectional SEM images of inverted MaPbI₃ solar cells based on 100 nm (a), 150 nm (b), and 500 nm (c) thick CBTS HTLs. Solar cells were stored in N₂ filled desiccator for three weeks.

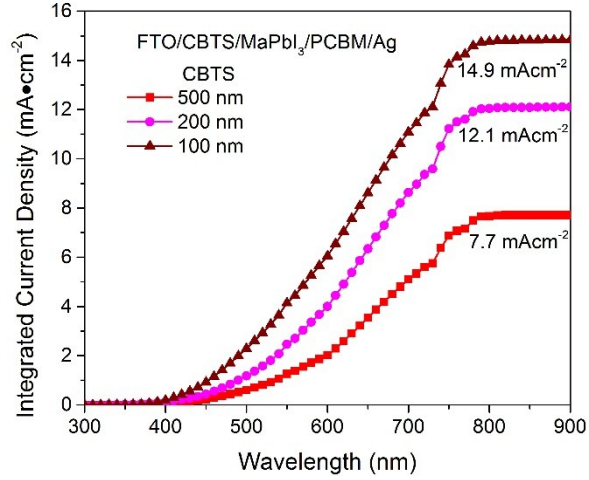


Figure S3 Integrated current densities from the EQE data of CBTS based inverted MaPbI₃ solar cells in Figure 5b.

Table S1 Device parameters under reverse ($V_{OC} \rightarrow J_{SC}$) and forward ($J_{SC} \rightarrow V_{OC}$) voltage scans of our best perovskite MaPbI₃ solar cells with various device structures.^a

Device Structure	Scan	PCE (%)	V_{OC} (V)	FF (%)	J_{SC} (mA cm ⁻²)
FTO/PEDOT:PSS/ MaPbI ₃ /PCBM/Ag	$V_{OC} \rightarrow J_{SC}$	8.5	0.927	66.69	13.75
	$J_{SC} \rightarrow V_{OC}$	8.1	0.924	65.52	13.38
FTO/MaPbI ₃ / PCBM/Ag	$V_{OC} \rightarrow J_{SC}$	3.5	0.684	50.05	10.15
	$J_{SC} \rightarrow V_{OC}$	2.5	0.673	45.85	8.22
FTO/TiO ₂ /MaPbI ₃	$V_{OC} \rightarrow J_{SC}$	14.2	1.04	74.12	18.42
/Spiro/Au	$J_{SC} \rightarrow V_{OC}$	13.5	1.04	68.51	18.80

^a These device parameters come from the light J-V curves given in Figure S3a.

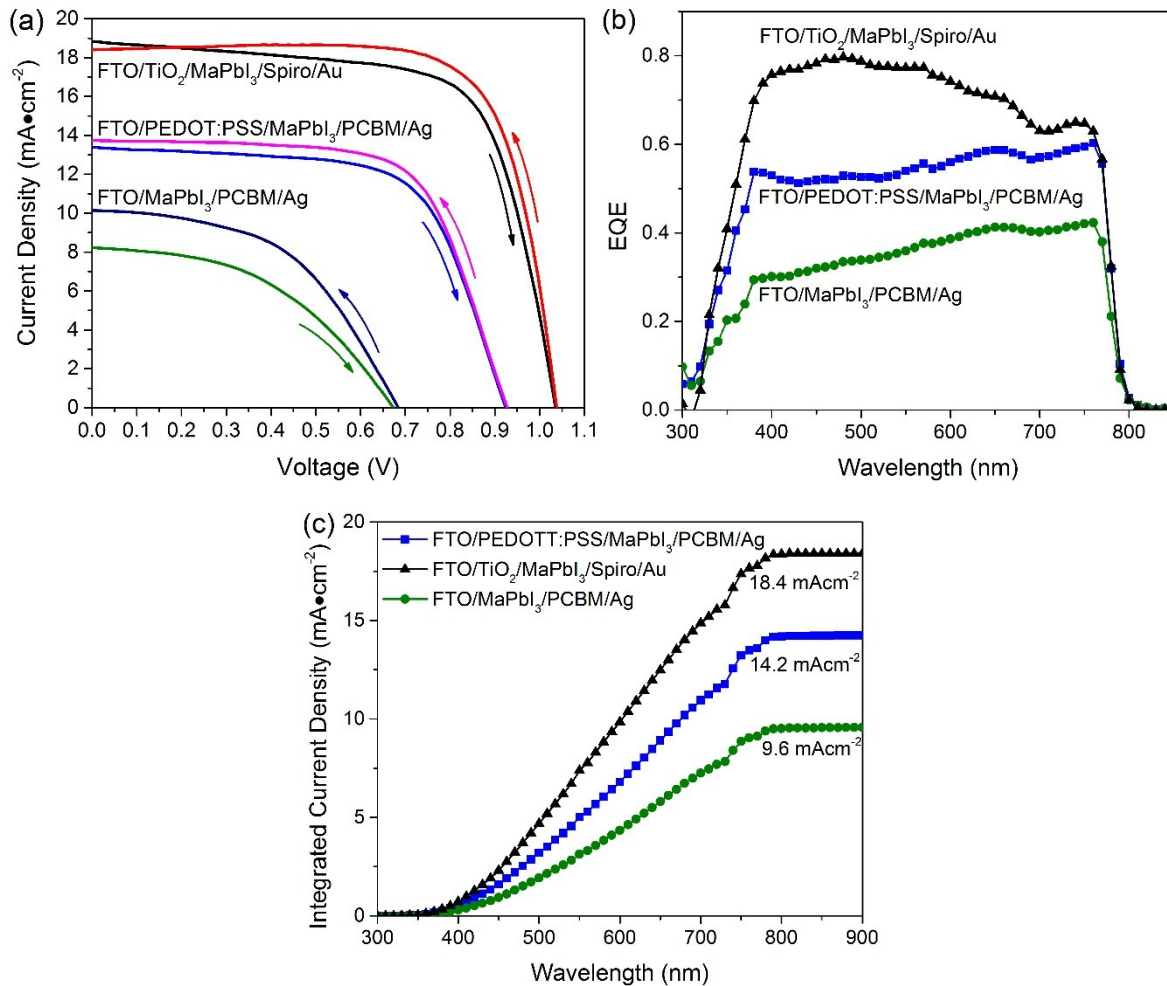


Figure S4 AM 1.5G illuminated J-V characteristics under reverse ($V_{OC} \rightarrow J_{SC}$) and forward ($J_{SC} \rightarrow V_{OC}$) voltage scans (a), corresponding EQE curves (b) and EQE integrated current densities (c) of our best MaPbI₃ solar cells with various device structures: FTO/PEDOT:PSS/MaPbI₃/PCBM/Ag, FTO/MaPbI₃/PCBM/Ag, and FTO/TiO₂/MaPbI₃/Spiro/Ag. Note: these devices were measured immediately as obtained under the ambient air condition (relative humidity: 70%).

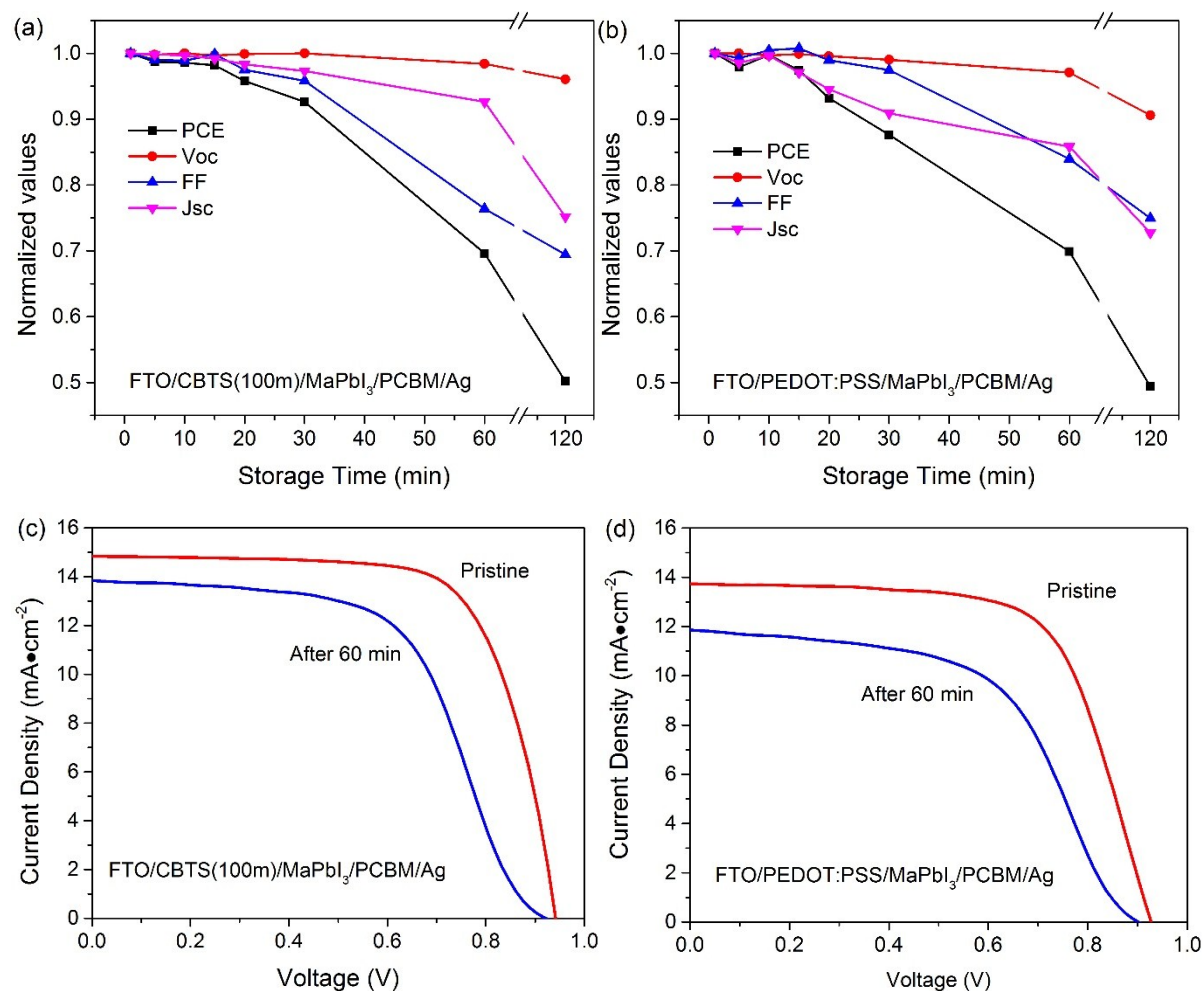


Figure S5 Device stability tests in the air for our best inverted MaPbI_3 solar cells based on a 100 nm CBTS (a) HTL and a PEDOTT:PSS HTL (b); light J-V curves of these two inverted MaPbI_3 solar cells based on CBTS (c) and PEDOTT:PSS (d), respectively. Note: device stability tests were measured under the ambient air condition (relative humidity: 70%).